RSC Advances




ROYAL SOCIETY OF CHEMISTRY

www.rsc.org/advances

**Graphical Abstract:**

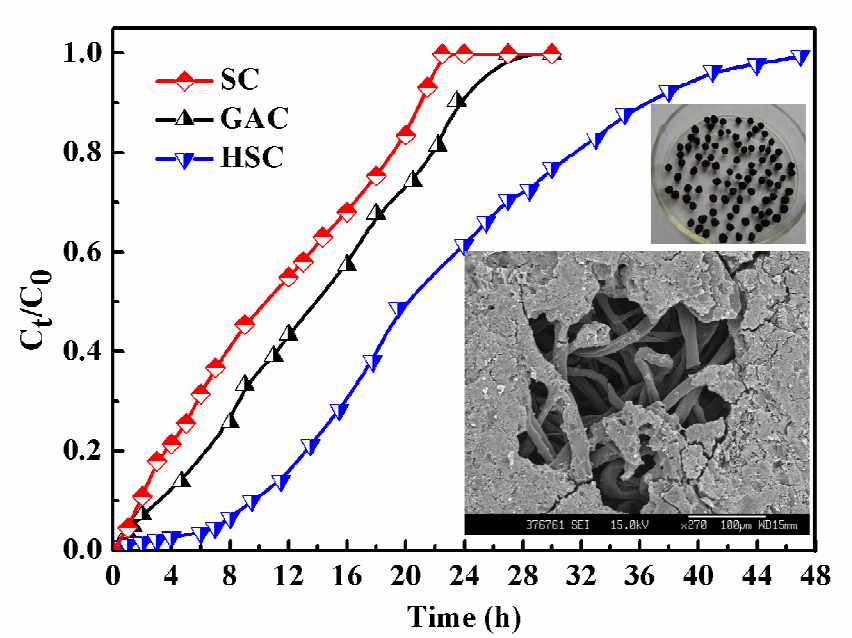


**Highlight:**

Hollow-like spherical sludge char (HSC) was prepared to decrease low pressure and increase high surface area to 1008 $m^2/g$.

Cite this: DOI: 10.1039/c0xx00000x

www.rsc.org/xxxxxx

PAPER

# Preparation and adsorption behavior of new hollow-like spherical sludge chars for methylene blue

**Zhijian Wu[a, b], Ya Xiong[a, d*], Guoqiang Guan[c], Lingjun Kong[a, e*], Shuanhong Tian[a, d]**

***Received (in XXX, XXX) Xth XXXXXXXXX 20XX, Accepted Xth XXXXXXXXX 20XX***

**DOI: 10.1039/b000000x**

A new pyrolytic process was successfully used to prepare hollow-like spherical sludge chars (HSC). In the process, pre-formed cotton spheres with a low density were firstly coated by a layer of sludge paste containing $ZnCl_2$ to form cotton fiber@ slugde sphere and then pyrolyzed at 500 $^oC$ for 2 h. The resulted HSC possessed a diameter of about 3 mm, a low density of 0.1008 g/cm$^3$ and a high surface area of 1008 m$^2$/g. The column adsorption behavior showed that the adsorption capacity and rate constant of HSC for methylene blue reached 186.4 mg/g and 0.232 mL/min mg. The adsorption capacity is about 8.4 and 12 folds of adsorption capacities of GAC (22.28 mg/g) and SC (15.26 mg/g), respectively, and the adsorption rate constant is about 1.3 folds of that of GAC and SC. The great adsorption capacity and rate constant can be considerably dependent on its special hollow-like spherical structure of HSC.

## Introduction

The sewage sludge is a complex mixture of organics (e.g., cellulose, humic substances and so on) and inorganics [1]. Its treatment and disposal have being become a world-wide issue due to the increased amount of sludge and the stringent environmental regulation all over the world. The application of traditional disposal options, including sanitary landfill, sea dumping, application to farmland and forestry, incineration frequently caused debate due to the potential of secondary pollution [2]. Carbonization of sludge for preparation of the available sludge chars is believed to be one of attractive disposal technologies for the sewage sludge [3].

Sludge char was firstly reported by Kemmer et al in 1971 [4]. After that, many papers have reported about the preparation of sludge derived char [5-10]. However, the sludge chars had low adsorption capacity due to the high ash content and low BET surface area [1, 3]. Recently, many new ways besides traditional activation methods have been developed to produce porous sludge chars with great surface area [11-15]. However, it is noticed that these sludge chars all have been used in the form of powers or granularity till now. They have some faults as adsorbents. For the sludge char powers, it is difficult to separate the sludge char powers from aqueous solution after they are used, and for the granular sludge chars, although they are easily separated from aqueous solution, the interior chars of these granularities act less because adsorption often occurs on the surfaces of adsorbents. Therefore, it is attractive to develop a new sludge char with the advantages in high availability and easy separation.

Hollow spheres have been attracted considerable interests in the past decades due to their well-defined morphology, low density, high surface area, surface permeability and potential applications in catalysis, photonic crystals, chromatography, protection of biologically active agents, fillers and waste removal etc [16-22]. However, to the best of our knowledge, there is still no report on hollow spherical sludge char.

Considering that template method is one of the preferable strategies for producing hollow spheres [23, 24], the method will be used to prepare hollow spherical sludge char in which pre-formed spheres with waste cotton fibers will be acted as the template. As shown in Fig. 1, the pre-formed cotton spheres were firstly coated with a layer of wet sludge paste added activation agent $ZnCl_2$, and then were pyrolyzed. Although the waste cotton spheres will be also carbonized together with sludge in the pyrolysis process and remained in spherical sludge chars, the interior cotton carbon will be much less compared with the sludge chars because the density of the waste cotton spheres is low. In other words, the resulted sludge chars will be possible hollow-like spheres, not complete hollow spheres.

The aim of this paper is to test the feasibility of the preparation strategy of the hollow-like spherical sludge char, as shown in Fig. 1, and to investigate its physical and chemical characteristics as well as adsorption performance for removal of organic pollutants in aqueous solution.

## Materials and Experiment

### Materials

Dewater sewage sludge containing 75 % $H_2O$ was obtained from the Liede sewage treatment plant (Guangdong, China). Cotton fiber was supplied by Jingke Instrument and Glassware Trading Company (Guangdong, China). The commercial activated carbon was obtained from Aladdin Industrial Corp.

Cite this: DOI: 10.1039/c0xx00000x

www.rsc.org/xxxxxx

PAPER

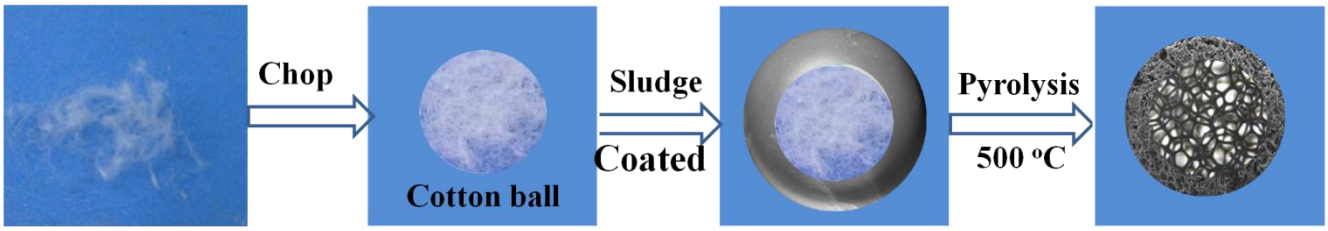


**Fig. 1.** Schematic diagram of the preparation process of hollow-like spherical sludge chars.

(Shanghai, China). Zinc chloride ($ZnCl_2$, AR) and methylene blue (MB) were all analytical grade. All water used in the experiments was deionized water.

**Preparation of hollow-like spherical sludge chars**

**Preparation of spherical sludge chars:** In order to impregnate well activated agent $ZnCl_2$, dewater sludge was mixed with $ZnCl_2$ solution at a solid-liquid ratio of 1 to 20, then being stirred overnight by a water-bath magnetic stirrer to form homogenous slurry and finally dried to homogenous pastes. The sludge pastes. The sludge pastes were directly pelletized into spheres in a diameter of about 4 mm and pyrolyzed at 500 °C for 2 h [25]. After cooling to room temperature, the product was washed with hydrochloric acid solution to remove inorganic compounds and then rinsed with deionized water until the pH reached 7. The obtained product was dried at 105 °C over night and named as SC.

**Preparation of hollow-like spherical sludge chars:** The hollow-like spherical sludge chars were prepared according to the process as shown in Fig. 1. The cotton fiber were mechanically tumbled into cotton spheres with a diameter of 4 mm, coated with the sludge pastes impregnated with $ZnCl_2$ in different mass ratios as described above. The mass ratio of cotton to sludge pastes was controlled to 1 to 2 based on weight basis, and the layer of the sludge paste was about 1 mm, and then being dried at 105 °C to form a kind of cotton@sludge sphere. Finally, the obtained spheres were put into ceramic ark, and heated in a programmable tube electric furnace (SKF-210, Hangzhou Lantian Instrument Co., China) at a rate of 20 °C $min^{-1}$ to 500 °C in the presence of $N_2$ holding for 2 h [25]. After cooling to room temperature, the product was washed with hydrochloric acid solution to remove inorganic compounds and then rinsed with deionized water until the pH reached 7. The obtained product was dried at 105 °C over night, the product with the optimal $ZnCl_2$ impregnation ratio was named as HSC.

**Design methodology of the preparation process optimization**

The experimental conditions of the above preparations were obtained by the following optimal processes. Impregnation ratio, i.g., the mass ratio of $ZnCl_2$ to dried sludge (*A*), pyrolysis temperature (*B*) and time (*C*) are regarded as the possible three main factors to affect the characteristics of sludge chars, according to the literatures [26]. The three factorial experiments with three levels (indicated as high, middle and low level) were designed to fit a model to data collected using a Box-Behnken response surface design. The specific surface area was used as the response for quantifying characteristics of the sludge chars. The model equation is constructed to use the coefficients to represent the relationship between the response and the factors. Full quadratic terms are included in the model, which is given as:

$$S_{BET} = f_0 + f_A A + f_B B + f_C C + f_{AA} A^2 + f_{BB} B^2 + f_{CC} C^2 + f_{AB} AB + f_{AC} AC + f_{BC} BC \quad (1)$$

where *A*, *B* and *C* are the factors of impregnation ratio, pyrolysis temperature and time, respectively, and their coefficients are represented as *f*s. The regression table summarized the estimated regression coefficients are used to evaluate the individual effects of the linear terms (*A*, *B* and *C*), the squared terms ($A^2$, $B^2$ and $C^2$) and the interaction terms (*AB*, *AC* and *BC*).

The design of experiments and statistical calculation was performed by using Minitab ® software (Minitab Inc., US). The Box-Behnken design was constructed to collect the experimental responses. The experiments were randomized with three center points and one replicate and their specifications are listed in the Table 1.

Table 1 Estimated regression coefficients for specific surface area.

| Term | | Coefficient | t | p |
|---|---|---|---|---|
| Constant | $f_0$ | 668.61 | 20.813 | 0.000 |
| *A*: Impregnation ratio | $f_A$ | 185.61 | 9.435 | 0.000 |
| *B*: Pyrolysis temperature | $f_B$ | -74.98 | -3.811 | 0.012 |
| *C*: Pyrolysis time | $f_C$ | -24.72 | -1.257 | 0.264 |
| $A^2$ | $f_{AA}$ | 4.88 | 1.619 | 0.166 |
| $B^2$ | $f_{BB}$ | -27.64 | -0.954 | 0.384 |
| $C^2$ | $f_{CC}$ | -56.02 | -1.935 | 0.111 |
| *AB* | $f_{AB}$ | -59.92 | -2.154 | 0.084 |
| *AC* | $f_{AC}$ | -11.10 | -0.399 | 0.706 |
| *BC* | $f_{BC}$ | 38.90 | 1.398 | 0.221 |

**Adsorption experiments**

The adsorption experiment was conducted in a fixed-bed column. It was made of a glass tube of 1.1 cm inner diameter and 28.5 cm height. A known quantity of the adsorbent was packed in

the column with the same bulk volume. Dye solution with a known concentration as pH 6.7 was pumped upward through the column at a desired flow rate controlled by a peristaltic pump (BL100-YZ15, PreFluid). The methylene blue solution at the outlet of the column was collected at regular time intervals and the concentrations ($C_t$, mg/L) were measured using a UV-visible spectrophotometer (Shimadzu U2010, Japan) at 665 nm. The total adsorption quantity can be calculated by integrating the adsorbed concentration ($C_0$-$C_t$, mg/L) versus t (h) plot. Total adsorbed quantity of methylene blue ($q_{total}$, mg) in the column for a given feed concentration ($C_0$, mg/L) and flow rate (Q, ml/min) is calculated as:

$$q_{total} = \frac{60 \times Q}{1000} \int_{t_0}^{t_{total}} (C_0 - C_t) dt = \frac{C_0 Q}{1000} \int_{t_0}^{t_{total}} (1 - \frac{C_t}{C_0}) dt \quad (2)$$

The maximum adsorption capacity of the column is defined by equations (3) as the total adsorbed methylene blue per gram of adsorbent ($w$) at the end of total flow time:

$$q_{eq} = \frac{q_{total}}{w} \quad (3)$$

### Characterization and analytical methods

The apparent density, also known as the bulk density, is an important characteristic of spherical activated carbon, being used for the determination of void fraction in packed column. The apparent density is measured according to the Chinese standard of GB/T 7702.4 [27], where the specified samples filled into a column of a known volume are weighed and the apparent density of the sample can be given as the ratio of weighted mass to known volume.

The pressure drop gives information about the permeability to flow of the bleaching fluid through the packing layer. The pressured drop over a packed column is adequately defined by a modified form of the semi-empirical Ergun equation [28]. In this study, the pressure drop is experimentally measured in the packed column with inner diameter of 11 mm and effective length of 300 mm. The deionized water flows through the packed column filled with the specified samples at three different flow rates. The pressure drops over the column are measured in the U-tube. All measurements are repeated for three times and their average and standardized derivation are calculated.

The specific surface area ($S_{BET}$) of the sample was determined by an auto-adsorption system (Auto-sorb-6, Quantachrome, USA) calculated based on the BET equation. The surface physical morphology of the sample was observed by the scanning electron microscopy (Hitachi S-2150, Japan). Themogravimetric (TG) analysis was carried out on a Thermogravimetry analyzer (TG209 F1, Netzsch, Germany).

## Results and discussion

### Optimization of HSC preparation process

Three factorial experiments with three levels (indicated as high, middle and low level) were designed to optimize the preparation process of HSC. In the optimization, specific surface area ($S_{BET}$) was used as the response term of three main experimental parameters including impregnation ratio ($A$), pyrolysis temperature ($B$) and pyrolysis time ($C$) since the value of $S_{BET}$ is an important indicator for sludge char absorbents.

Table 1 presents the estimated regression coefficients for $S_{BET}$ from the pyrolytic experiments of Box-Behnken design. It can be seen from the table that only the coefficients of constant ($f_0$), impregnation ratio ($f_A$) and pyrolysis temperature ($f_B$) have the p-values of over 0.05 among the statistical results. The result indicates that only the constant and linear terms of $A$ and $B$ have significant effects on the $S_{BET}$, and all the squared and interaction terms can be ignored in the estimation of response. Among the significant factors, the impregnation ratio ($A$) was found to have the greatest influence on the $S_{BET}$ of the sludge char, and increased $A$ will lead to an increase in the $S_{BET}$. The pyrolysis time ($C$) and interaction factors ($AB$, $AC$ and $BC$), however, seemed to have minor impacts on the $S_{BET}$.

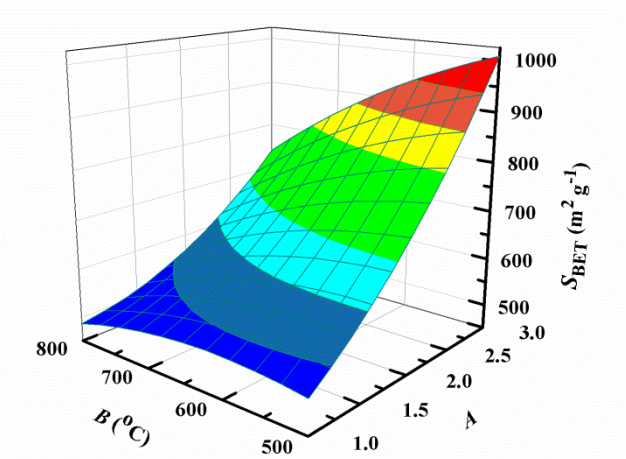


**Fig. 2.**Three-dimensional response of specific surface area for 2 h pyrolysis.

Fig. 2 presents the three-dimensional response of specific surface area to two factors of impregnation ratio ($A$) and pyrolysis temperature ($B$) for 2 h pyrolysis. It was found that the $S_{BET}$ increased with impregnation ratio ($A$), however, the increased degree is rather diverse for different pyrolysis temperatures. The increased degree of $S_{BET}$ for the low temperature is much greater than that for high temperature. For instance, a near two-fold increase of $S_{BET}$ (from 517 to 1008 $m^2/g$) was found for the pyrolysis temperature of 500 ℃ when the impregnation ratio rised from 1.0 to 3.0, but only one half increase was observed at 800 ℃. The negative effect of high pyrolysis temperature is due to the collapse of porous structure [29]. Combining with experimental data in Fig. 2, the optimal impregnation mass ratio of $ZnCl_2$ to dried sludge and pyrolysis temperature are controlled 3.0 and 500 °C, respectively, for HSC preparation in this work.

### Characterization of hollow-like sludge char

Fig. 3 presents the photos and SEM of HSC prepared at the optimal condition. HSC is a black spherical material with a diameter of about 3 mm (Fig. 3a) and an apparent core@shell structure (Fig. 3b). Its interior core is cotton carbon fibers (Fig. 3b), and its out shell is porous sludge chars (Fig. 3c and d).

Cite this: DOI: 10.1039/c0xx00000x

www.rsc.org/xxxxxx

PAPER

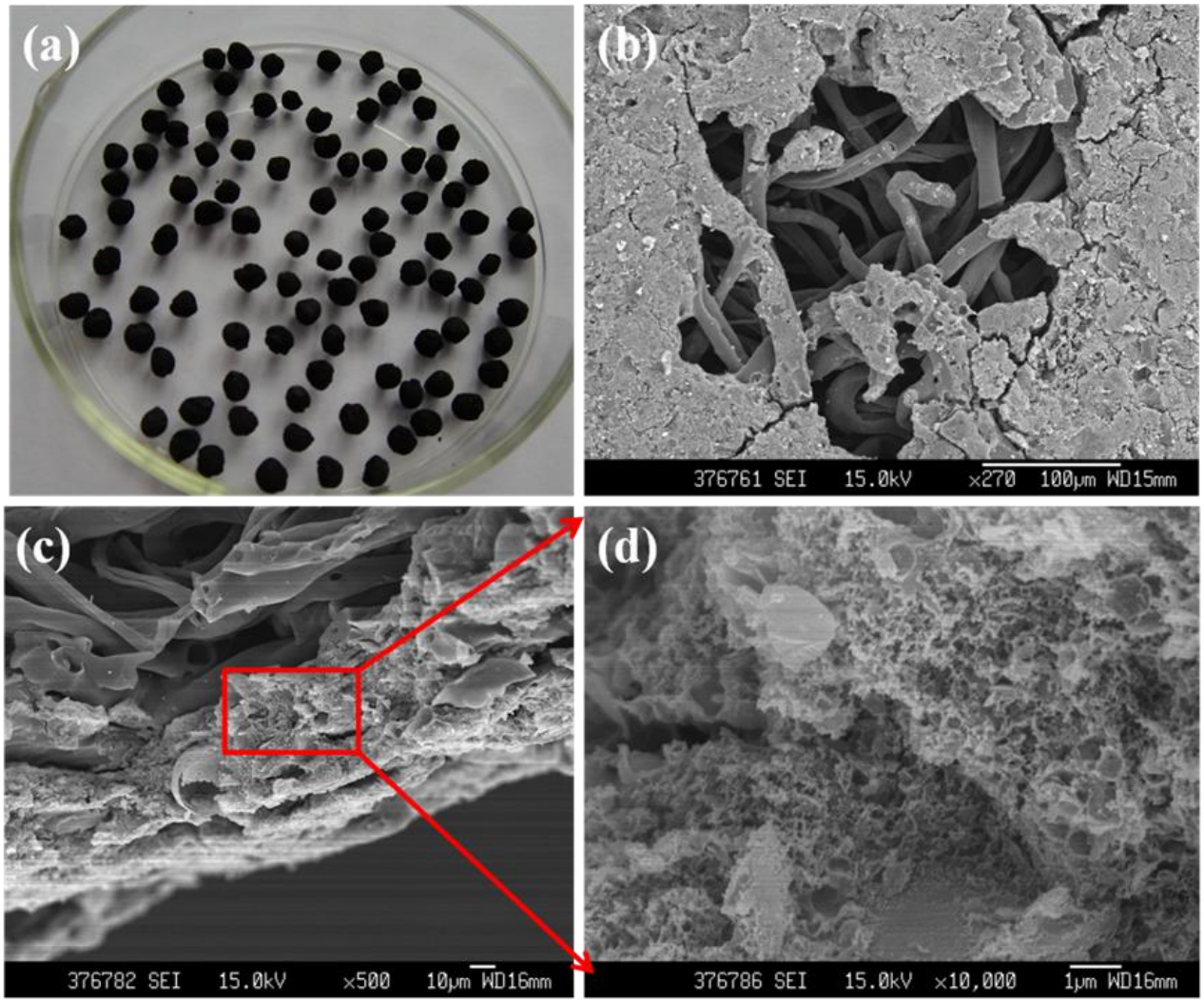


**Fig. 3.** (a) photos of HSC, (b) SEM of the open section of HSC, (c) SEM of the shell of HSC and (d) partition magnification SEM of the shell.

However, the cotton carbon fiber looks like sparse, therefore, HSC is inferred to possess a hollow-like spherical structure. The deduction was further confirmed by TG data of cotton and sludge. As shown in Fig. 4, the weight loss of sewage sludge was 37.8% while that of cotton reached 82.7% at 500 $^{o}$C. Because cotton spheres were coated by sewage sludge with the weight ratio of 1: 2 before pyrolysis, the weight ratio of the inner cotton carbon fibber and sludge char after pyrolysis was calculated to be 1:7.2 in HSC, according to the above weight loss ratio at 500 $^{o}$C. In other word, the weight percentage of interior cotton char was only 12.2% of HSC weight, while the interior volume of HSC was estimated about 81 %. However, the diameter of HSC was about 3 mm while the thickness of the shell was about 0.1 mm measured by the Fig. 3 (c). It is easy to calculate that the volume percentage of the cotton char fiber core was 81 % although its mass percentage was only about 12.2 %. Therefore, it is reasonable to refer the HSC as hollow-like spherical sludge char. The yield of HSC was about 47 %. Although it is a little lower than the yield of the common sludge carbon (about 55 %), its carbon content is high than that of the latter.

Table 2 $S_{BET}$ and packing properties of GAC, SC and HSC.

| Samples | Apparent density (g/cm$^3$) | $S_{BET}$ (m$^2$/g) | Pressure drop at varied flow rate (mm $H_2O$) | | |
|---|---|---|---|---|---|
| | | | 10 ml/min | 20 ml/min | 30 ml/min |
| GAC | 0.5469±0.0058 | 1087.5 | 55.3±5.2 | 89.9±1.8 | 121.2±0.3 |
| SC | 0.6613±0.0084 | 470.1 | 61.1±8.6 | 110.5±11.2 | 169.3±4.0 |
| HSC | 0.1008±0.0038 | 1008.4 | 38.8±11.2 | 66.3±15.8 | 94.0±16.7 |

Table 2 lists the $S_{BET}$ of GAC, SC and HSC. Their $S_{BET}$ were 1087.5, 470.1 and 1008.4 m$^2$/g, respectively. Normally, the $S_{BET}$

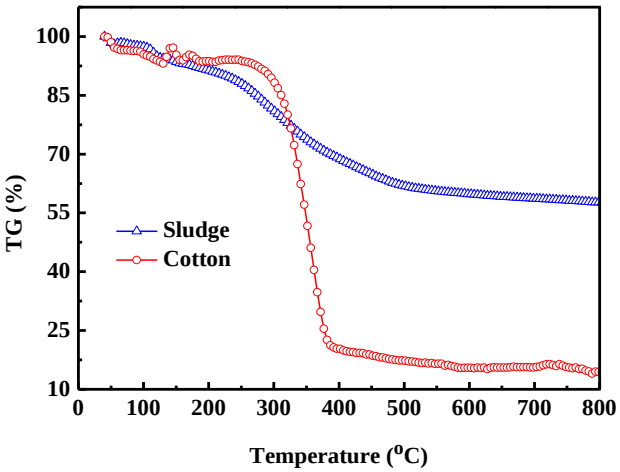


**Fig. 4.** Thermal gravimetric curves of sewage sludge and cotton.

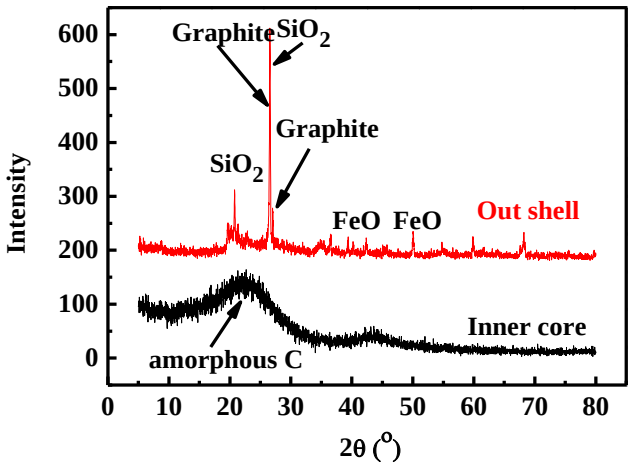


**Fig. 5.** XRD patterns of out shell and inner core of HSC.

of HSC could be equal to the sum of $S_{BET}$ of cotton carbon fiber and SC in the HSC according to their mass percentage. Considering that the mass percentage of the sludge char and cotton carbon fiber in HSC are 87.8% and 12.2%, respectively, while the $S_{BET}$ of cotton carbon fiber was 2150.6 $m^2/g$ (not shown in this paper), the $S_{BET}$ of HSC can be calculated as 675.1 $m^2/g$. The calculated $S_{BET}$ of HSC is clearly less than the experimental $S_{BET}$ of HSC. The fact shows that hollow-like sphere possesses the advantage of great surface area.

Table 2 also lists the apparent densities of GAC, SC and HSC. It can be seen from the table that the apparent densities of HSC was only 18 % and 15 % of those of GAC and SC, respectively. The low apparent density will result in a less resistant loss in the filling absorbent column, as shown as data of the pressure drop in Table 2. This is another advantage of the hollow-like spherical sludge char.

The composition of the out shell and inner core of HSC was highly different (as shown in Fig. 5 and Table 3). The inner core of HSC was mainly amorphous carbon and the out shell of HSC was composed of $SiO_2$ and graphite carbon, as shown in Fig. 5. In addition, elemental analysis (Table 3) showed that the carbon content of the sludge out shell was only 12.14%, much lower than to 84.65% of inner core of HSC. The ratios of C/N and C/H of out shell were also lower than those of inner core. This indicated that the carbonization of inner cotton is high than that of sludge char out shell.

Table 3 Element analysis of out shell and inner core of HSC compared to GAC.

| Samples | C % | H % | N % | C/N | C/H |
|---|---|---|---|---|---|
| shell | 12.14 | 1.663 | 1.21 | 10.07 | 7.30 |
| core | 84.65 | 2.059 | 0.11 | 782.88 | 41.10 |
| GAC | 89.54 | 1.780 | 0.16 | 570.95 | 50.30 |

### Adsorption performance of HSC for methylene blue

Three column reactors packed with GAC, SC and HSC fillers, respectively, were used to compare the adsorption performances of these fillers for methylene blue in aqueous solution. Their adsorption breakthrough curves for the various experimental conditions (Table 3) were presented in Fig. 6. As illustrated in Fig. 5, the half breakthrough time was 13.9, 10.6 and 20.2 h, respectively, when the $C_t/C_0$ was 0.5. The adsorption capacities of GAC and SC were calculated to be 22.28 and 15.26 mg/g, respectively. They were similar to the results reported in the literatures [30]. However, the adsorption capacity of HSC (186.42 mg/g) was about 8.4 and 12.2 times of those of GAC and SC although the $S_{BET}$ of GAC was equal to HSC. Such great disparity between the adsorption capacities of HSC and those of GAC and SC to methylene blue can be contributed to the hollow-like structure of HSC since the hollow-like structure took the advantages in penetrability as discussed above.

Table 4 Column data parameters of methylene blue adsorption onto varied adsorbents.

| Adsorbents | Packed mass (g) | Half breakthrough time (h) | $q_{total}$ (mg) | $q_e$ (mg/g) |
|---|---|---|---|---|
| GAC | 15.14 | 13.9 | 337.3 | 22.28 |
| SC | 17.78 | 10.6 | 271.4 | 15.26 |
| HSC | 2.82 | 20.2 | 525.7 | 186.42 |

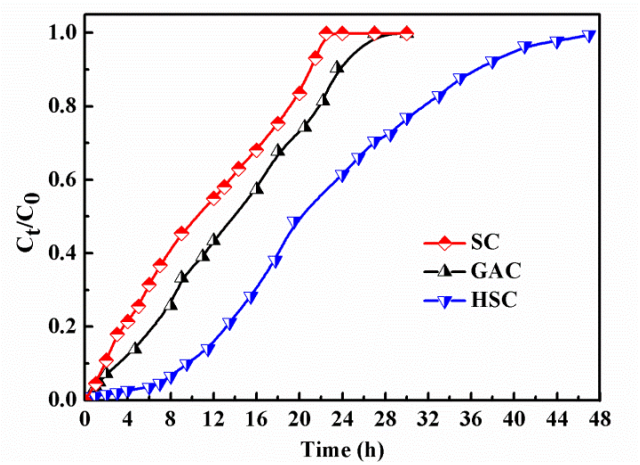


**Fig. 6.** Adsorption breakthrough curves of G-CAC, G-SC and G-HSC to methylene blue ($C_0$=150 mg/L, Q=163.22 ml/h).

In order to further understand the adsorption performance of HSC, two common models were used to evaluate the adsorption

Cite this: DOI: 10.1039/c0xx00000x

www.rsc.org/xxxxxx

PAPER

Table 5 Dynamic adsorption model parameters of methylene blue on varied adsorbents.

| Adsorbents | Thomas model | | | Yoon-Nelson model | | |
|---|---|---|---|---|---|---|
| | $k_{Th}$ (mL/min mg) | $q_0$ (mg/g) | $R^2$ | $k_{YN}$ (mL/g min) | $\tau$ (h) | $R^2$ |
| GAC | 1.253 | 22.16 | 0.983 | 0.188 | 13.69 | 0.983 |
| SC | 1.227 | 14.67 | 0.979 | 0.184 | 10.65 | 0.979 |
| HSC | 1.547 | 169.40 | 0.985 | 0.232 | 19.50 | 0.985 |

dynamic parameters. The first model is Thomas model as follows [31]:

$$\ln(\frac{C_0}{C_t}-1)=\frac{k_{Th}q_0w}{Q}-k_{Th}C_0t \quad (4)$$

where $k_{Th}$ is the Thomas rate constant (mL/h mg), $q_0$ is the equilibrium adsorption capacity (mg/g), $C_0$ is the initial concentration of MB (mg/L), $C_t$ is the outlet concentration at time t (h), w is the mass of adsorbent (g), Q is the flow rate (mL/h). The values of $k_{Th}$ and $q_0$ of the three absorbents were all obtained by fitting their breakthrough curves with Thomas model and shown in Table 5. As can be seen from Table 5, the $q_0$ values (22.16, 14.67 and 169.40 mg/g) of GAC, SC and HSC were all consistent with their experimental values (Table 4). The fact shows that Thomas model can describe the adsorption breakthrough curves of HSC to MB well. As we know, Thomas model is suitable for the adsorption processes where the external and internal diffusions are absent [31-33], therefore, the fitting result indicates that the adsorption of HSC to MB is not limited by diffusion. The result is consistent with the high surface permeability of hollow-like spherical structures for HSC.

The second model used for fitting the adsorption breakthrough curve is Yoon-Nelson model [34]. The linearized Yoon-Nelson model could be expressed as follows:

$$\ln\frac{C_t}{C_0-C_t}=k_{YN}t-\tau k_{YN} \quad (5)$$

where $k_{YN}$ is the rate velocity constant, $\tau$ is the half breakthrough time (h). The values of $k_{YN}$ and $\tau$ can be calculated from the slope and intercept of the linear plot for Yoon-Nelson model. As shown in Table 5, the correlation coefficients were ranged from 0.98 to 0.99. More important, the calculated $\tau$ of G-CAC, G-SC and G-HSC were 13.69, 10.65 and 19.50 h, respectively. They were high consistent with the experimental half-breakthrough time (Table 4), indicating that the adsorption breakthrough curves of GAC, SC and HSC are all described well with Yoon-Nelson model. By comparing the $k_{YN}$ as shown in Table 5, it can be seen that the $k_{YN}$ of HSC was 0.232, being about 1.3 time of the $k_{YN}$ of GAC, SC. The fact further suggests that the hollow-like spherical structure of HSC is much beneficial to the mass transport of methylene blue.

In addition, the adsorption of real wastewater on HSC was also conducted with the sewage from Datansha sewage treatment plant, Results shown that about 86.7 % COD could be removed from 100 ml sewage with a initial COD concentration of 252 mg/L and 0.5 g HSC. The removal efficiency is higher 50 % and 80 % than that of GAC and SC, respectively. The result showed that HSC is also an efficient material for removal of real sewage.

**Regeneration of HSC**

The yield of exhausted HSC was 97 % after column adsorption experiment, indicating that the weight loss of the HSC was only about 3 %, further suggesting that the HSC was mechanical stability after cyclic usage. Thermal treatment at 500 °C was conducted to regenerate the exhaust HSC. Fig. 7 shows the adsorption amounts of the virgin and regenerated HSC for methylene blue (150 mg/L) in a bath reactor. Although the adsorption amount of methylene blue decreased with the increase in the generation number, it still kept about129 mg/g after regeneration for 2 cycles. It was observed that the adsorption capacity of the HSC after 2 time regeneration was decreased by about 14% when no $ZnCl_2$ was added in the regeneration process. However, the adsorption capacity basically kept unchanged when $ZnCl_2$ was added in the regeneration process. The slight decrease of adsorption amount is possible due to the pore blocking up by the methylene blue carbonized substance.

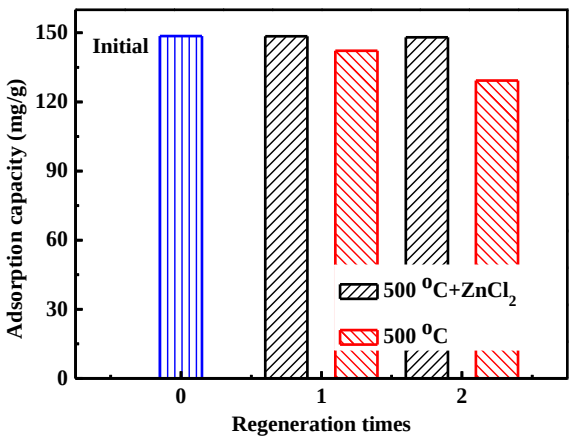


**Fig. 7.** Adsorption amounts of methylene blue at initial concentration of 150 mg/L on HSC after thermal regeneration.

## Conclusions

Hollow-like spherical sludge chars with a diameter of about 3 mm were prepared by pyrolysis of the pre-formed cotton fiber@sludge sphere at 500 $^{o}$C with the cotton sphere as template. These sludge chars possessed a low density of 0.1008 g/cm$^3$, a high surface area of 1008 m$^2$/g, a great adsorption capacity of 186.4 mg/g and a great adsorption rate constant of 0.232 mL/min mg towards methylene blue. The excellent performance of these sludge chars can be contributed to its special hollow-like spherical structure.

## Acknowledgements

This research was supported by Nature Science Foundations of China (20977117, 21107146), Nature Foundations of Guangdong Province (92510027501000005), Science and Technology Research Programs of Guangzhou City (2012J4300118) and Project of Education Bureau of Guangdong Province (cgzhzd1001), the Fundamental Research Funds for the Central Universities (121pgy20).

## Notes and references

[a] *School of Environmental Science and Engineering, Sun Yat-Sen University, Guangzhou 510275, P.R. China; E-mail: cesxya@mail.sysu.edu.cn (Ya Xiong)*

[b] *Guangzhou sewage purification co.,LTD., Guangzhou, Guangdong, P. R. China, 510655*

[c] *School of Chemistry and Chemical Engineering, Southern China University of Technology, Guangzhou, Guangdong, P. R. China, 510640*

[d] *Guangdong Provincial Key Laboratory of Environmental Pollution Control and Remediation Technology, Guangzhou 510275, P.R. China*

[e] *School of Environmental Science and Engineering, Guangzhou University, Guangzhou 510275, P.R. China; E-mail: kongl_jun@163.com (Lingjun Kong).*

1 L. Gu, N.W. Zhu, H.Q. Guo, S.Q. Huang, Z. Y. Lou, H. P. Yuan, *J. Hazard. Mater.*, 2013, **246-247**, 145.

2 F. Wang, K. Shih, X. W. Lu, C. S. Liu, *Environ. Sci. Technol.*, 2013, **47**, 2621.

3 L. Gu, N. W. Zhu, D. F. Zhang, Z. Y. Lou, H. P. Yuan, P. Zhou, *Bioresour. Technol.* 2013, **136**, 719.

4 F. N. Kemmer, S. R. Robertson, R. D. Mattix, U.S. Pattent 1971. No. 3,619,420.

5 N. R. Khalili, M. Campbell, G. Sandi, J. Golas, *Carbon*, 2000, **38**, 1905.

6 A. Bagreev, D. C. Locke, T. J. Bandosz, *Ind. Eng. Chem. Res.*, 2001, **40**, 3502.

7 T. J. Bandosz, K. A. Block, *Ind. Eng. Chem. Res.*, 2006, **45**, 3666.

8 M. Seredych, T. J. Bandosz, *Ind. Eng. Chem. Res.*, 2007, **46**, 1786.

9 C. V. Gómez-Pacheco, J. Rivera-Utrilla, M. Sánchez-Polo, J. J. López-Peñalver, *J. Hazard. Mater.*, 2012, **217-218**, 76.

10 S. Athalathil, F. Stüber, C. Bengoa, J. Font, A. Fortuny, A. Fabregat, *J. Hazard. Mater.*, 2014, **267**, 21.

11 L. J. Kong, S. H. Tian, R. S. Luo, W. Liu, Y. T. Tu, Y. Xiong, J. Chem.Technol. Biotechnol. 2013, **88**, 1473.

12 K. M. Smith, G. D. Fowler, S. Pullket, N. J. D. Graham, Water Res., *2009*, **43**, 2569.

13 Q. Augustine, B. Rajasekhar, *Chem. Eng. J.*, 2011, **170**, 194.

14 L. Gu, Y. C. Wang, N. W. Zhu, D. F. Zhang, S. Q. Huang, H. P. Yuan, Z. Y. Lou, M. L. Wang, *Bioresour. Technol.*, 2013, **146**, 779.

15 L. J. Kong, Y. Xiong, S. H. Tian, R. S. Luo, C. He, H. B. Huang, *Bioresour. Technol.*, 2013, **146**, 457.

16 J. P. Kathleen, S. J. Jules, M. Edith, *Nature*, 1994, **367**, 258.

17 L. X. Zhang, Y. X. Sun, W. B. Jia, S.S. Ma, B. Song, Y. Li, H. F. Jiu, *Ceram. Int. Part A*, 2014, **40**, 8897.

18 A. D. Dinsmore, M. F. Hsu, M. G. Nikolaides, M. Marquez, A. R. Bausch, D. A. Weitz, *Science*, 2002, **298**, 1006.

19 L. Guo, L. Zhang, J. Zhang, J. Zhou, Q. He, S. Zeng, X. Cui, J. Shi, *Chem. Commun.*, 2009, **40**, 6071.

20 J. Qian, F. Wu, *J. Mater. Chem. B*, 2013, **1**, 3464.

21 X. D. Ma, X. Feng, J. Guo, H. Q. Cao, X. Y. Suo, H. W. Sun, M. H. Zheng, *Appl. Catal. B: Environ.*, 2014, **147**, 666.

22 H. J. Lee, S. Choi, M. Oh, *Chem. Commun.*, 2014, **50**, 4492.

23 J. Hu, M. Chen, X. Fang, L. Wu, *Chem. Soc. Rev.*, 2011, **40**, 5472.

24 X. W. Lou, C. L. Yuan, L. A. Archer, *Adv. Mater.* 2007, **19**, 3328.

25 F. Rozada, M. Otero, A. Morán, A.I. García, *Bioresour. Technol.*, 2008, **99**, 6332.

26 S. Rio, C. Faur-Brasquet, C. L. Le, P. Courcoux, C. P. Le, *Chemosphere*, 2005, **58**, 423.

27 Standard test method for packing density of granular activated carbon from coal. GB/T 7702.4-1997.

28 S. Ergun, *Chem. Eng. Prog.*,1952, **48**, 89.

29 H-L. Chiang, K-H. Lin, H-H. Chiu, *J. Hazard. Mater.*, 2012, **229–230**, 233.

30 F. Rozada, L. F. Calvo, A. I. García, J. Martín-Villacorta, M. Otero, *Bioresour. Technol.*, 2013, **87**, 221.

31 H. C. Thomas, *J. Am. Chem. Soc.*, 1944, **66**, 1466.

32 Z. Aksu, F. Gonen, *Process Biochem.*, 2004, **39**, 599.

33 T. Mitra, B. Singha, N. Bar, S.K. Das, *J. Hazard. Mater.*, 2014, **273**, 94.

34 Y. H. Yoon, J. H. Nelson, *Am. Ind. Hyg. Assoc. J.*, 1984, **45**, 509.